Journal of Energy Chemistry 26 (2017) 919–926

Contents lists available at ScienceDirect

Journal of Energy Chemistry

journal homepage: www.elsevier.com/locate/jechem

http://www.journals.elsevier.com/journal-of-energy-chemistry/

Thermokinetic and conductivity analyzes of the high CO_2 chemisorption on Li_5AlO_4 and alkaline carbonate impregnated Li_5AlO_4 samples: Effects produced by the use of CO_2 partial pressures and oxygen addition

Pedro Sánchez-Camacho, J. Francisco Gómez-García, Heriberto Pfeiffer*

Laboratorio de Fisicoquímica y Reactividad de Superficies (LaFReS), Instituto de Investigaciones en Materiales, Universidad Nacional Autońoma de Meźico, Circuito exterior s/n, Cd. Universitaria, Del. Coyoacań C.P. 04510, Ciudad de Meźico, Mexico

ARTICLE INFO

Article history:
Received 22 March 2017
Revised 11 May 2017
Accepted 22 May 2017
Available online 30 May 2017

Keywords:
CO_2 capture
Thermogravimetric analysis
Partial pressure
Ionic conduction

ABSTRACT

The effect of CO_2 partial pressure was evaluated during the CO_2 chemisorption in penta lithium aluminate (Li_5AlO_4), using different CO_2 and O_2 partial pressures in the presence or absence of alkaline carbonates. Results showed that using low P_{O_2} (0.1) did not affect the kinetic and final CO_2 chemisorption process. Moreover, small additions of oxygen ($P_{O_2}=0.05$) into the mixture flue gas, seemed to increase the CO_2 chemisorption. Additionally, the presence of alkaline carbonates modified the CO_2 capture temperature range. CO_2 chemisorption kinetic parameters were determined assuming a double exponential model where direct CO_2 chemisorption and CO_2 chemisorption controlled by diffusion processes are considered. Finally, ionic diffusion was analyzed by ionic conduction analysis, where all the gravimetric and ionic measurements were in good agreement showing different diffusion processes depending on temperature. Finally, the oxygen and alkaline carbonate additions have positive effects during the CO_2 chemisorption process in Li_5AlO_4, and a possible reaction mechanism is presented.

1. Introduction

Carbon dioxide (CO_2) is considered to be the main contributor of the global warming, and due to this problem it is necessary to reduce the amounts of these emissions. Moreover, it is important to separate it from exhaust gases, developing effective CO_2 separation techniques and CO_2 sorbents [1]. Therefore, CO_2 capture and storage (CCS) technologies have attracted interest to reduce the increasing amount of CO_2 released into the atmosphere. CCS involves capturing the CO_2 emitted by power plants and other industrial operations and permanently storing it deep underground [2].

On the other hand, the removal of CO_2 has also been used to improve the hydrogen production in a steam methane reforming (SMR) system, called sorption enhanced steam methane reforming (SE-SMR), which is operated at temperatures between 500 and 700 °C. In this process, a CO_2 captor is installed together with the catalyst in the reactor bed for removal of CO_2 from the gas phase, showing several advantages compared to conventional steam methane reforming, among them, high-purity H_2 production (>95%). High-temperature sorption, using solid sorbents, is a good choice in the application fields mentioned above, compared with current low-temperature methods, such as amine-based absorption, because these processes work at high operation temperatures, where the flue gas does not need to be cooled prior to chemisorbing CO_2 [3–7].

Among the various high-temperature solid sorbents that have been studied, different lithium-containing ceramics have been proposed as possible CO_2 captors. Li_4SiO_4 [8–12], Li_2CuO_2 [1,13,14], Li_2ZrO_3 [15–18], Li_5AlO_4 [19,20] and Li_8SiO_6 [12,21–23], among others, are all examples of ceramic sorbents with interesting capture properties from the point of view of high CO_2 capture capacities, high carbonation reaction rates at elevated temperatures and in some cases, good stabilities and cyclic properties.

Among all these lithium-based materials, lithium aluminate (Li_5AlO_4) has attracted increasing attention in different research fields for its high lithium density [19,20,24]. Li_5AlO_4 ceramic presents two different crystal polymorphs α-Li_5AlO_4 and β-Li_5AlO_4, where both polymorphs have orthorhombic crystal structures. As CO_2 captor, both phases have been tested by Pfeiffer and coworkers [19,20], demonstrating that β-Li_5AlO_4 crystal phase presents better chemisorption properties, being able to trap CO_2

* Corresponding author.
E-mail addresses: pfeifferperea@gmail.com, pfeiffer@iim.unam.mx (H. Pfeiffer).

http://dx.doi.org/10.1016/j.jechem.2017.05.008
2095-4956/

chemically in the temperature range from 200 to 700 °C (reaction 1) and have good cyclability characteristics.

$$Li_5AlO_4 + 2CO_2 \rightarrow 2Li_2CO_3 + LiAlO_2 \quad (1)$$

The sorption process consists of a rapid superficial CO_2 chemisorption stage and a much slower ion-diffusion-controlled stage, meaning that once CO_2 reacts with Li_5AlO_4 on the solid surface to completely form an external shell composed of Li_2CO_3 and $LiAlO_2$, the Li^+ and O^{2-} ions should diffuse through the product layer to the surface to continue reacting with CO_2 [8,25]. The secondary phase, $LiAlO_2$, does not react with CO_2 due to thermodynamic factors. However, when $LiAlO_2$ is contained in the external shell, it promotes the lithium ionic diffusion into the Li_2CO_3–$LiAlO_2$ external shell at temperatures higher than 600 °C. Moreover, the lithium carbonate formation implies that one of each four oxygen atoms, present originally in the Li_5AlO_4 ceramic, must become part of the Li_2CO_3. Consequently, these oxygen atoms must diffuse as well. So, the presence of this gas in the whole reactive atmosphere would modify the reaction kinetics [26].

The reaction stage of CO_2 chemisorption in Li_5AlO_4 is a gas–surface reaction, and the sorption kinetics determined in other lithium-based materials as Li_4SiO_4 [5], Na_2ZrO_3 [27,28] or Li_2ZrO_3 [3,29] are relatively poor at low CO_2 partial pressure ($P_{CO_2} < 0.5$), owing to less molecular collision and taking more time to attain satisfactory sorption conversions. Iwan et al. [3] concluded that there is a linear relationship between the apparent reaction rate and the carbon dioxide partial pressure. Because the CO_2 concentration of flue gases in power plants or SE-SMR is only 4–20 vol%, and gas cannot remain in reactors for a long time because of the high flowrate; there is an urgent need to obtain sorbents with fast and stable cyclic kinetics of sorption/desorption at low CO_2 partial pressure.

A part form that, the CO_2 capture of some lithium ceramics has been modified by the addition of different alkaline carbonates, which favours the formation of eutectic phases on the carbonate external shell [10]. In fact, Li_5AlO_4 has shown variations on its CO_2 capture temperature range, depending on the alkaline carbonate [10,30]. Moreover, it has been reported in literature the use of alkaline carbonate molten phases for different applications, and it has been reported that the specific Li_2CO_3:Na_2CO_3:K_2CO_3 = 42.5:32.5:25 mol% mixture presents one of the lowest melting points (~400 °C) [31].

Therefore, the aim of the present work was to analyze the CO_2 chemisorption process on Li_5AlO_4 varying different physicochemical conditions such as the CO_2 and O_2 partial pressures as well as the alkaline carbonate addition to pristine Li_5AlO_4. The present work was performed using different techniques for the kinetic analysis and for the sample and diffusion characterization.

2. Experimental

Li_5AlO_4 was synthesized by solid state reaction using lithium oxide (Li_2O, Aldrich) and aluminum oxide (Al_2O_3, Aldrich). Initially, powders were mechanically mixed and pressed into pellets (10 MPa). Subsequently, the pellets were heated to 900 °C for 12 h and rapidly cooled to room temperature. Lithium was used in excess (10 wt%), due to its tendency to sublimate. In addition, part of the sample was mixed with an eutectic molten carbonate mixture composed of Li_2CO_3, Na_2CO_3 and K_2CO_3 with a mole percent ratio of 42.5/32.5/25 mol%, which presents a melting point at around 400 °C [31].

X-ray diffraction (XRD) patterns were obtained from a diffractometer (Bruker AXS, D8 Advance) coupled to a copper anode X-ray tube. Li_5AlO_4 and other crystalline phases were identified by their corresponding Joint Committee Powder Diffraction Standards (JCPDS) files. Nitrogen adsorption–desorption isotherms and BET surface area analyzes were performed using a Minisorp II instrument, from the Bel-Japan. These experiments were performed at 77 K, using a multipoint technique, where samples were previously degassed at room temperature for 24 h in vacuum. The BET model was used to determine the corresponding surface areas.

Different thermal analyzes were performed using a Q500HR instrument from TA Instruments. Initially, a set of samples was dynamically heated from room temperature to 850 at 3 °C/min, using a mixture flow containing different CO_2 concentrations (Praxair, grade 3.0) in N_2 balance atmosphere (Praxair, grade 4.8). Subsequently, other dynamic experiments were performed adding O_2 (Praxair, grade 3.0) to the CO_2/N_2 mixture flow. The partial pressures of CO_2 and O_2 were determined by its fraction of the total feed flow rate and the total pressure. The total feed flow was always set at 60 mL/min. Afterwards, the samples were tested isothermally at different temperatures (between 650 and 750 °C) in presence of the same mixture flows. For the isothermal experiments, each sample was heated to the corresponding temperature into a N_2 flux. Then, once the temperature was reached, the gas was switched from N_2 to the different mixture flows.

Electrical measurements on Li_5AlO_2 and $LiAlO_2$ samples were performed by impedance spectroscopy with a Precision Impedance Analyzer 6500B Wayne Kerr Electronics, in order to determine the lithium ion diffusion properties. Colloidal platinum (Tanaka Kikinzoku Kogyo K.K.) was used on samples as electrodes. Those electrodes were annealed at 600 °C for 2 h before the electrical measurements. Impedance spectra were collected in the 40 Hz–10 MHz range at 500 mV. The electrical measurements were accomplished by cooling in the temperature range 800–200 °C in a quartz cell coupled with a vacuum pump, the pressure inner cell was 30 Pa. The temperature inside the cell was monitored with a K-type thermocouple. For each single data point, the equilibrium time was 2 h. Each impedance spectrum was fitted to a single RC circuit using the software Zview®.

3. Results and discussion

Fig. 1(a) shows the powder X-ray diffraction (XRD) measurements of Li_5AlO_4, which confirmed the purity of the sample. The diffraction pattern fitted to the JCPDS file 70-0432, which corresponds to Li_5AlO_4 with an orthorhombic crystalline structure. In addition to the Li_5AlO_4 structural characterization, some microstructural properties were evaluated by N_2 adsorption-desorption (Fig. 1(b)). According to the IUPAC classification, the Li_5AlO_4 sample showed an adsorption isotherm type II, corresponding to non-porous material [32]. Additionally, this sample presented a very narrow H3 hysteresis loop, which may have produced a few mesoporous due to a partial particle sintering. The BET surface area was found to be equal to 0.8 m^2/g.

After the sample characterization, different dynamic TG experiments were performed, varying the CO_2 partial pressure (Fig. 2). The P_{CO_2} was varied from 1 to 0.1, and as it can be seen, all the thermograms presented the same thermal trend and very similar weight increments. Between room temperature and 100 °C all the samples lost around 1 wt%, which can be attributed to water desorption. Then, two different weight increments were evidenced between 300–500 °C and 550–720 °C. As in previous Li_5AlO_4–CO_2 reports [19], these weight increments are attributed to the superficial and bulk CO_2 chemisorptions on Li_5AlO_4 and other alkaline ceramics. Only small weight differences are observed in these thermograms during the superficial CO_2 chemisorption (see square inset of Fig. 2), where the thermogram corresponding to a $P_{CO_2} = 1$ gained around 2–3 wt% more CO_2 than $P_{CO_2} = 0.1$. The other visual difference is observed at temperatures higher than 700 °C, as the final weight increment was slightly better when the P_{CO_2} was

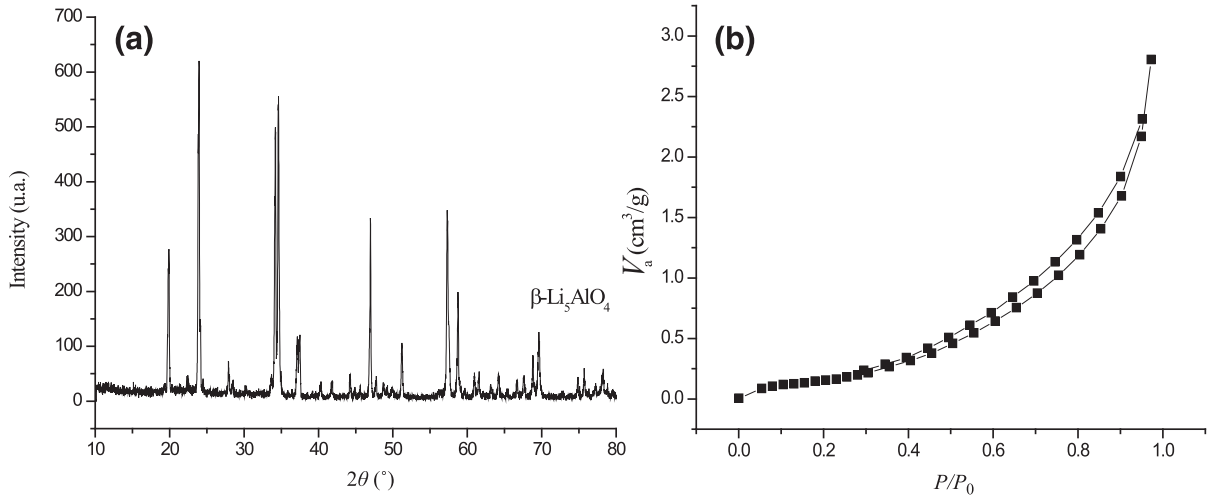

Fig. 1. (a) XRD pattern of the Li_5AlO_4 sample, which fitted to the 70-0432 JCPDS file; (b) N_2 adsorption-desorption isotherm of the Li_5AlO_4 sample.

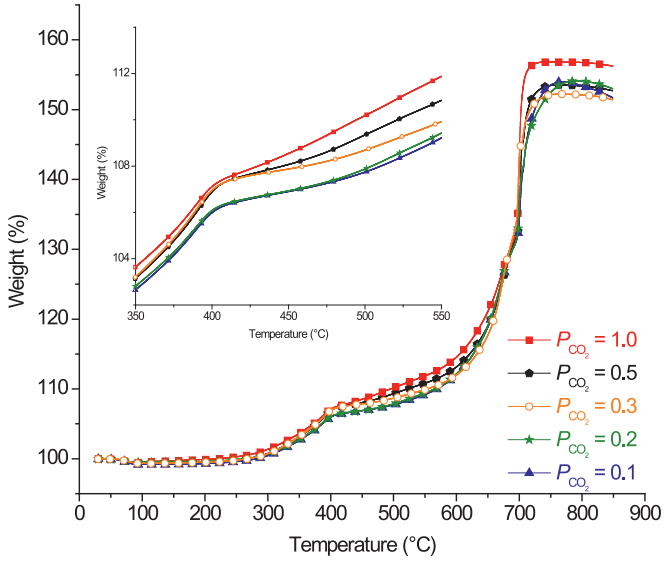

Fig. 2. Dynamic thermogravimetric analysis of Li_5AlO_4 using different P_{CO_2} (1.0, 0.5, 0.3, 0.2 and 0.1). The square inset shows the superficial CO_2 chemisorption section.

1.0. These effects may be associated to different solid-gas equilibriums produced by the CO_2 partial pressure. Nevertheless, further isothermal analyzes were performed in order to better understand and explain these results.

Fig. 3 shows five different isothermal sets, where P_{CO_2} (0.5, 0.3, 0.2 and 0.1) is compared as a function of temperature (650, 675, 700, 725 and 750 °C). As it could be expected, the weight increments and kinetic behaviors importantly changed as a function of temperature. However, the CO_2 chemisorption trends varied as a function of P_{CO_2} in two different ways; at moderate temperatures (650 and 675 °C) and at $T \geq 700$ °C. At moderated temperatures, the lowest P_{CO_2} (0.1) depicted a slightly higher CO_2 capture after three hours, although their kinetic behaviors, at short times, were not the best ones. For example, at 675 °C the final weight increments were 43, 34, 39 and 41 wt% with P_{CO_2} of 0.1, 0.2, 0.3 and 0.5, while the CO_2 capture after 150 s was 15, 10, 26 and 33 wt% for the same partial pressures. It seems that in this temperature range the so called CO_2 chemisorption controlled by diffusional processes is promoted at low P_{CO_2}. It may be explained due to Li_5AlO_4 sintering process during the heating process. Previous works have reported that Li_5AlO_4 powders tend to sinter between room temperature and 675 °C [19], which is in good agreement with the results reported here. Moreover, using different P_{CO_2} may induce different external shell compactions due to variations on the chemisorption-desorption equilibrium, favoring or not, the formation of a Li_2CO_3–$LiAlO_2$ porous or texturized external shell and consequently the gas diffusion processes [33].

The behavior described above for the moderate temperatures was not evidenced at $T \geq 700$ °C (see Fig. 3(c)–(e)). In these cases, the three isothermal sets presented a linear trend, where the CO_2 chemisorbed increased as a function of the P_{CO_2}. The main difference observed in these isotherms was produced at short times, where the CO_2 chemisorption is faster at higher P_{CO_2}. In this case, the Li_5AlO_4 original phase and carbonated external shell are already sintered and the presence of any kind of porosity is not favored. Thus, the CO_2 chemisorption depends of inter- and/or intracrystalline diffusion processes.

As it was already mentioned in the introduction section, and according to reaction (1), the CO_2 chemisorption in Li_5AlO_4 not only depends on the CO_2 concentration, but on the lithium and oxygen mobility. Lithium atoms have to diffuse from the Li_5AlO_4 phase to the Li_2CO_3, but part of the oxygen present in Li_5AlO_4 structure has to diffuse as well to the lithium carbonate. Thus, the CO_2 chemisorption process on Li_5AlO_4 may depend of lithium and oxygen diffusion processes. Based on that, different dynamic and isothermal thermograms were performed with the following gas mixture partial pressures $P_{CO_2}/P_{O_2} = 0.2/0.05$ or 0.2/0.2, balanced with N_2. Fig. 4 shows the dynamic and isotherms (700 °C) thermogravimetric comparisons of the CO_2 chemisorptions for these experiments in the absence and presence of oxygen (with two different P_{O_2}), which are compared with the CO_2 saturated experiments. From these thermograms, it is evident that oxygen addition did modify the CO_2 chemisorption in Li_5AlO_4, in addition to the CO_2 partial pressure described above. According to the TG dynamic experiments, oxygen addition only enhances the CO_2 chemisorption at low partial pressures ($P_{O_2} = 0.05$) between 500 and 700 °C. In fact, the isothermal experiments performed at 700 °C clearly show how low P_{O_2} addition improves the CO_2 capture synergistically to the partial pressure effect. Since the capture in a P_{CO_2}/P_{O_2} atmosphere of 0.2/0.2 was lower than that presented by CO_2 saturated and the lowest P_{O_2} atmospheres, it was supposed that in this gas mixture oxygen must compete and saturate the Li_5AlO_4 surface, reducing the CO_2 chemisorption.

Based on previous results, different isothermal experiments were performed at 700 °C and $P_{O_2} = 0.05$, varying P_{CO_2} (Fig. 5), as this P_{O_2} improved the CO_2 chemisorption. All the isotherms pre-

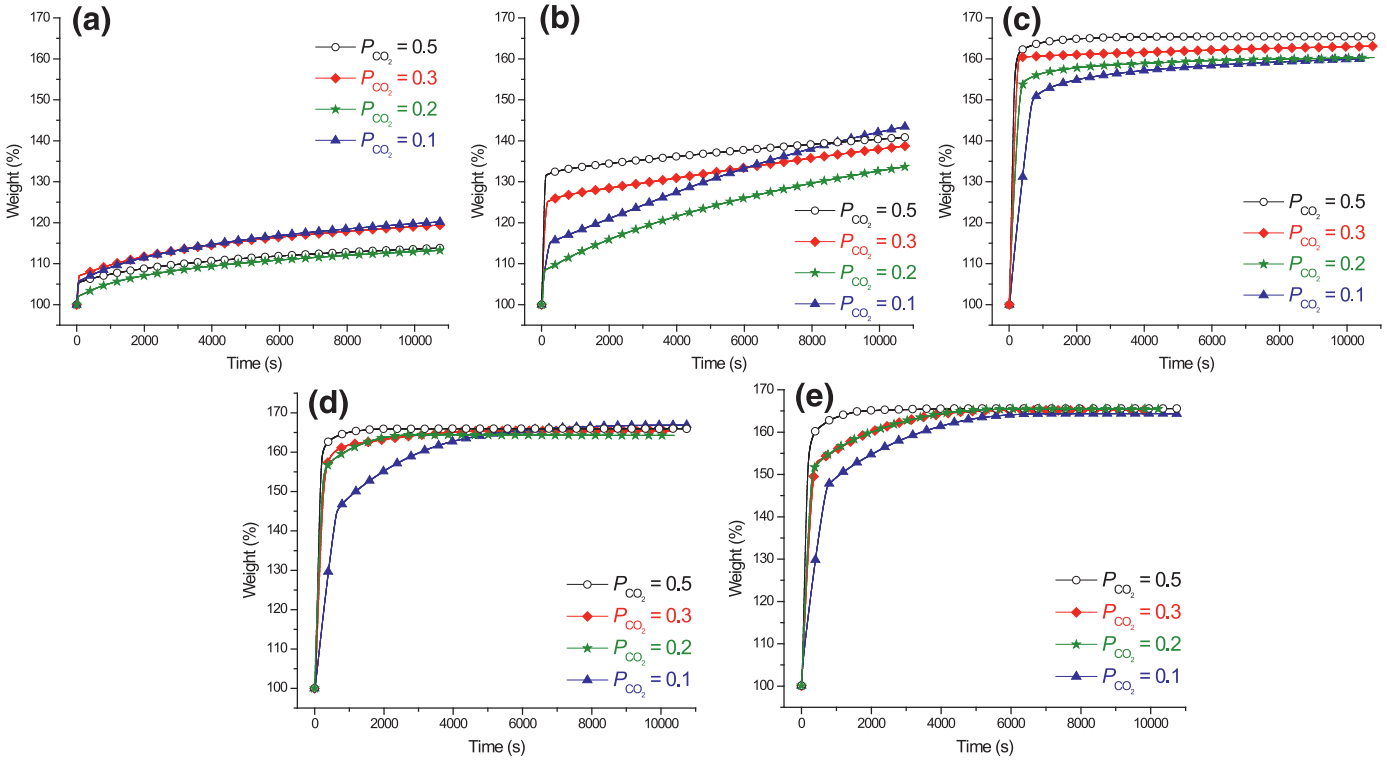

Fig. 3. Chemisorption thermogravimetric isotherms performed with different P_{CO_2} at 650 (a), 675 (b), 700 (c), 725 (d) and 750 °C (e).

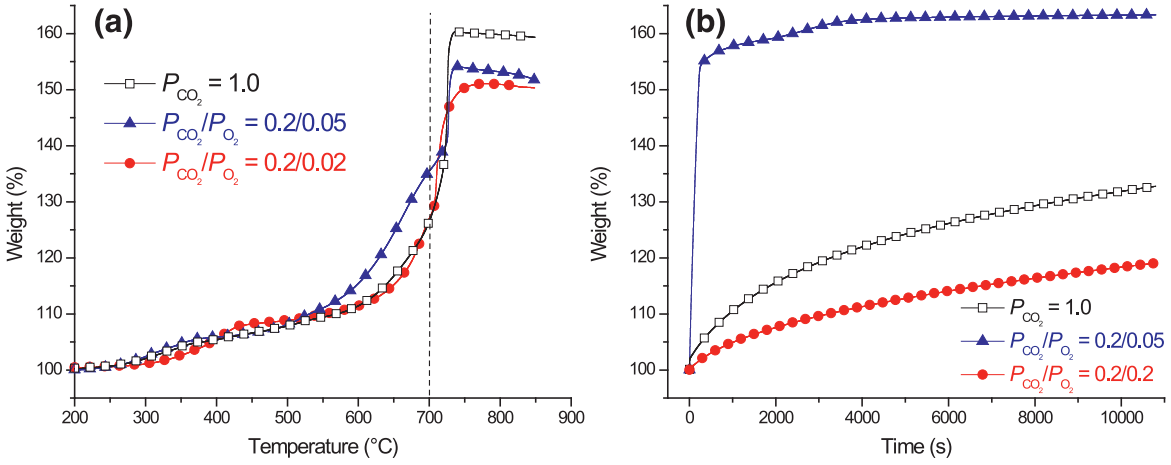

Fig. 4. Dynamic and isothermal (700 °C) thermogravimetric analyzes of Li_5AlO_4 comparing the presence, or not, of oxygen at different concentrations in the gas mixture flow.

sented the same exponential behavior, where most of the CO_2 capture is produced in the first moments. Nevertheless, isotherms where oxygen was present were faster than those obtained in the oxygen absence, and the amounts of CO_2 captured did not vary in more than 2 wt%. In order to further analyze these isotherms, with and without O_2, all of them were fitted to the double exponential model, as in previous works related to Li_5AlO_4 and other lithium ceramics [8,11,25,26]. The double exponential model is:

$$y = A\exp(-k_1 t) + B\exp(-k_2 t) + C \quad (2)$$

where y represents the weight percentage of CO_2 chemisorbed, t is the time, and k_1 and k_2 are the exponential constants for the Li_5AlO_4–CO_2 chemisorption over the particle surfaces and the CO_2 chemisorption kinetically controlled by diffusion processes. The kinetic parameters obtained at each temperature and P_{CO_2} are presented in Table 1, and compared with the corresponding val-

Table 1. Kinetic parameters of Li_5AlO_4 with different P_{CO_2} isotherms fitted to a double exponential model.

T (°C)\P_{CO2}	0.1	0.2	0.3	0.5
k_1 (s^{-1}, $\times 10^{-3}$)				
650	0.78	0.77	0.68	0.72
675	0.19	3.57	14.61	18.26
700	2.79	5.89	8.39	10.76
700 + O_2	6.49	9.23	10.3	26.46
725	3.05	8.24	6.38	9.29
750	2.91	7.04	6.09	9.02
k_2 (s^{-1}, $\times 10^{-3}$)				
650	0.09	0.06	0.05	0.06
675	0.001	0.11	0.03	0.04
700	0.21	0.21	0.04	0.63
700 + O_2	0.13	0.43	0.49	0.43
725	0.41	1.12	0.46	0.87
750	0.45	0.52	0.55	1.04

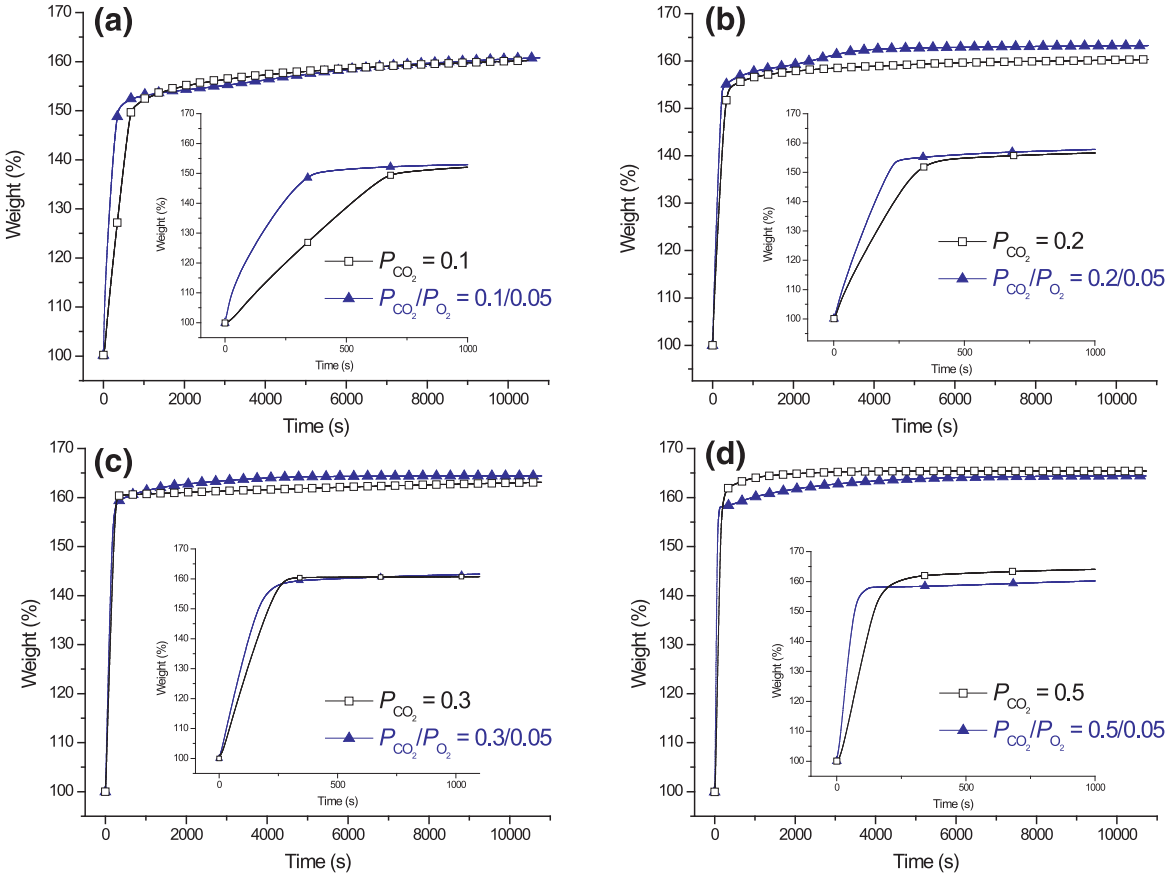

Fig. 5. Chemisorption thermogravimetric isotherms performed at 700 °C, using a P_{O_2} equal to 0.05, while the P_{CO_2} was varied. The square insets show the first reaction moments of the corresponding isotherm.

ues in the presence of oxygen (P_{O_2}). In general, these results evidence that k_1 values (direct CO_2 chemisorption in Li_5AlO_4 particle surfaces) are one order of magnitude higher than k_2 values (CO_2 chemisorption kinetically controlled by diffusion processes). This is a typical behavior observed for the CO_2 capture process in alkaline ceramics at high temperatures [8,11,25,26]. Thus, k_2 value indicates that the diffusion processes are the limiting process. In that sense, when oxygen was added to the gas flow, the k values presented the following tendency: Direct CO_2 chemisorption in Li_5AlO_4 particle surfaces was improved by the oxygen addition (independently of the P_{CO_2}) while CO_2 chemisorption kinetically controlled by diffusion processes did not follow any specific trend. Based in these results, it seems that the presence of oxygen facilitates the carbonate formation over the particle surface. Thus, oxygen present in the gas mixture must react with lithium and CO_2, producing Li_2CO_3. Latter, structural oxygen must be realized at a slower kinetic rate. However, once the Li_2CO_3–$LiAlO_2$ external shell is formed the oxygen presence does not enhance the CO_2 chemisorption process. It can be related to lithium and oxygen diffusion constant values, which must be lower than the oxygen addition in the direct CO_2 chemisorption process. In fact, the k_2 values support this idea.

In order to understand the kinetic variations, it should be mentioned that carbon dioxide reacts with oxygen and lithium ions from Li_5AlO_4 surface to yield $LiAlO_2$ and Li_2CO_3 according with reaction (1). This reaction creates atomic vacancies at the Li_5AlO_4 surface, which can be occupied by the structural ions from the bulk material, inducing a diffusion process, or part of the vacancies may be used for the oxygen adsorption and dissociation. In the bulk, the oxygen vacancies rearrange themselves to lead a tetrahedral corner sharing network of [AlO_4] that is the essential structure form for $LiAlO_2$ crystal phase and differs from the not linked [AlO_4] tetrahedrons in Li_5AlO_4 crystal phase. On the other hand, when oxygen is present in the gas mixture, the Li_5AlO_4 carbonation reaction would continue through the O_2 adsorption and dissociation, facilitating the carbonation process, as the anionic diffusion, from the Li_5AlO_4, is not required. Here, oxygen adsorption-dissociation may be induced by the acid-base interaction produced between oxygen and oxygen surface vacancies. In such a case, only lithium atoms have to diffuse, and the oxygen atoms can be realized at any time without affecting the carbonation process. This reaction scheme is represented in the Fig. 6.

Based on the previous results, and trying to improve the CO_2 chemisorption on Li_5AlO_4, a mixture of alkaline carbonates was incorporated to the sample trying to enhance the different diffusion processes due to the melting of this eutectic phase, these results are presented through dynamic experiments in Fig. 7(a) and isothermal experiments in Fig. 7(b). In the dynamic experiments, it is observed that the carbonates mixture diminished the superficial capture at low CO_2 partial pressures, but at elevated temperatures it had a positive effect due to the formation of the eutectic carbonate phase resulting in a higher CO_2 capture. In Fig. 7(b) all the isothermal experiments performed at 700 °C reached the kinetic equilibrium unlike the same experiments without the presence of carbonates. As it was already mentioned, the formation of the eutectic phase allows the CO_2 diffusion into the material at lower temperatures (Fig. 8). Is easy to see that the maximum capture takes place at temperatures higher than 700 °C when the system does not have carbonates, and it drops below 700 °C when carbonates are present. In addition, the carbonates did not modify significantly the total CO_2 capture.

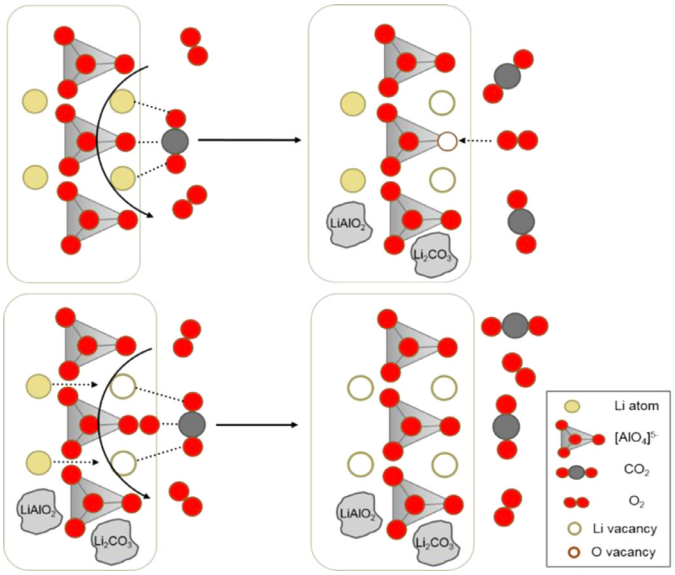

Fig. 6. Scheme representing the initial Li_5AlO_4 carbonation process, in the presence of oxygen.

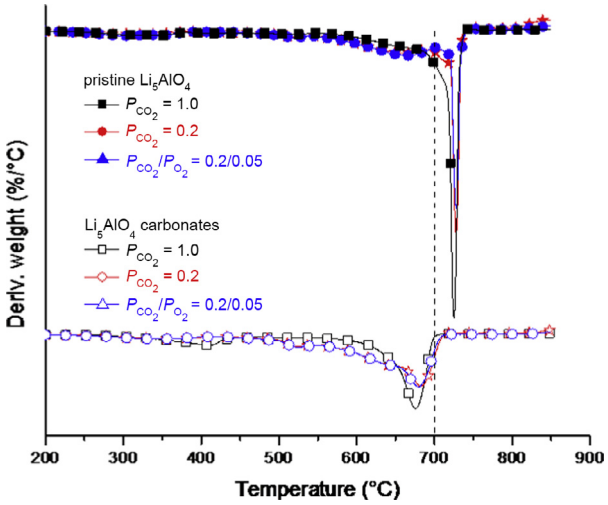

Fig. 8. DTG curves for thermogravimetric analyzes of Li_5AlO_4 with and without alkaline carbonates under different CO_2 and O_2 partial pressures.

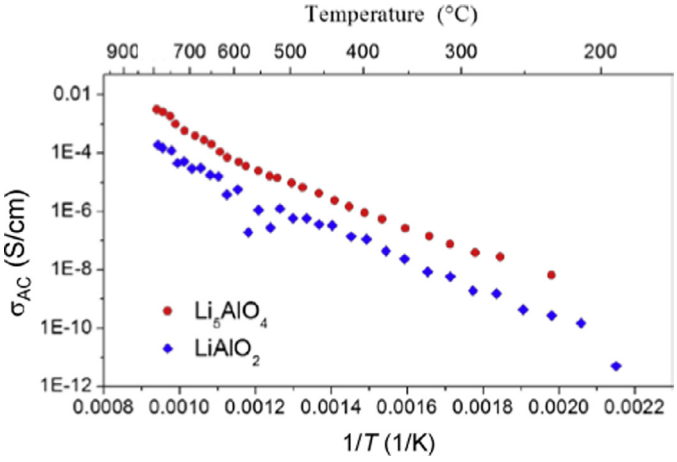

Fig. 9. AC conductivity for Li_5AlO_4 (blue points) and $LiAlO_2$ (red points) samples.

Based in all these results, it has been shown that lithium and oxygen diffusion processes are important factors in the Li_5AlO_4–CO_2 chemisorption process, where these two atoms have to diffuse in different crystalline phases such as Li_5AlO_4, $LiAlO_2$ and Li_2CO_3. Based in this statement, the ionic conductivity of Li_5AlO_4 and $LiAlO_2$ was analyzed. Fig. 9 shows the electrical conductivity of Li_5AlO_4 and $LiAlO_2$ samples. Li_5AlO_4 displays the highest electrical conductivity in all temperature range. The $LiAlO_2$ conductivity behavior shows a considerably noise in the measurements obtained between 500 and 600 °C. This effect could be due to the $\alpha \rightarrow \beta$ crystal $LiAlO_2$ phase transition [34]. The Li_5AlO_4 conductivity behavior does not display any noise that could be due to some crystal phase change. In this way, we can observe the electrical behavior only for the monoclinic β phase. Electrical transport commonly depends of two main contributions: electronic and ionic. $LiAlO_2$ and Li_5AlO_4 compounds do not have free electrons, so the electronic contribution can be neglected and the ionic conduction will be the only contribution in electrical properties.

The electrical conductivity (σ_T) is related to the ions diffusion through the Nernst–Einstein equation (Eq. (3)), where c_i refers to the number of charge carriers in the system, q_i is the electrical charge for a specific charge carrier, D_i is the pre exponential diffusion constant for a specific charge carrier, E_a is called activation energy and represents the energy of a bulk diffusion process, k_B is

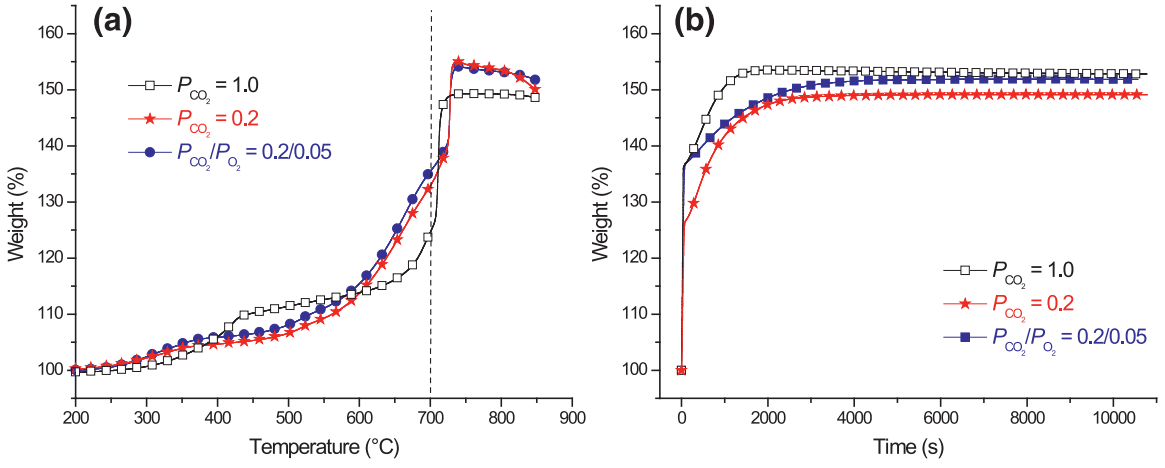

Fig. 7. Dynamic and isothermal (700 °C) thermogravimetric analyzes of Li_5AlO_4 with alkaline carbonates under different CO_2 and O_2 partial pressures.

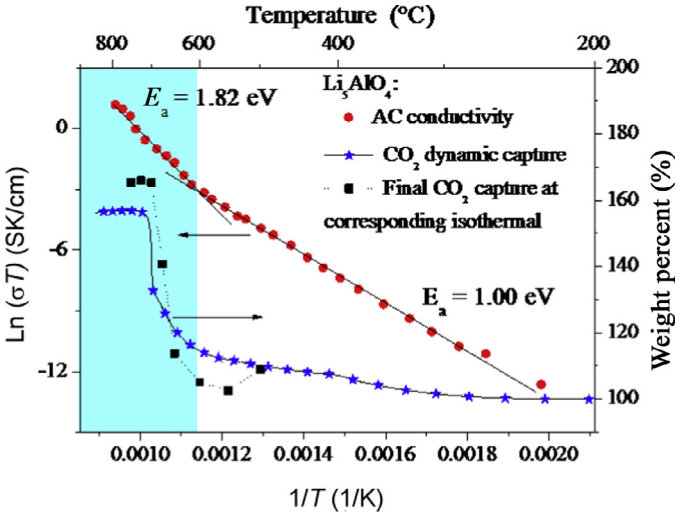

Fig. 10. Activation energy curves for Li_5AlO_4 ionic transport (red points). Also the CO_2 thermogravimetric dynamic and isothermal captures are presented, for comparison purposes.

the Boltzmann constant and T is the absolute temperature.

$$\sigma_T = \sum \frac{c_i q_i^2}{k_B T} D_i \exp\left(\frac{-E_a}{k_B T}\right) \quad (3)$$

As the CO_2 capture process at high temperature is associated to lithium and oxygen diffusion into the crystal [35], it is possible to obtain the E_a from the electric measurements and correlates with the CO_2 capture properties of Li_5AlO_4 [36]. In order to know the E_a in Li_5AlO_4 compound, ln (σT) vs $1/T$ plot is used (Fig. 10), where Li_5AlO_4 conductivity is presented and it is possible to observe two different regions, depicted by linear behaviors. Each linear trend corresponds to two different ionic transport mechanisms. At $T < 600$ °C, there is an ionic transport mechanism with an E_a equal to 1.00 eV, while at $T > 600$ °C the E_a is 1.82 eV. These E_a values are indicative that the ionic transport specie responsible is the O^{2-} ion. In fact, the E_a values presented by Li_5AlO_4 are similar to those reported by Al_2O_3 for O^{2-} conductivity [37]. Moreover, the activation energy values reported for Li-ion conductors are importantly lower (~0.3 to 0.57 eV [38]), in comparison to the values obtained here. Hence, as both E_a can be associated to O^{2-} mobility (Fig. 10), the change in E_a at 600 °C could be due to the change in the number of O^{2-} carriers. At low temperatures, the number of charge carriers remains constant and it is associated to intrinsic crystal defects, the E_a displayed is associated only with ions migration. As temperature rises, the number of charge carrier increases because there is enough energy to create more charge carrier, and the E_a displayed by the sample depends of the ions migration plus the energy to creates new defects (charge carriers) [39]. In this context, the Li_5AlO_4 conductivity could be associated to intrinsic defects at $T < 600$ °C and to new defects at $T > 600$ °C.

To correlates the electrical behavior with the Li_5AlO_4–CO_2 capture properties, the Fig. 10 shows the electrical and different CO_2 capture results; the dynamic weight increment and the final weight increments observed at each isothermal experiment. As the CO_2 capture process depends on lithium and oxygen diffusion through crystal structure, it could be possible that at $T < 600$ °C the CO_2 capture was controlled by diffusion via intrinsic defects. In this way, the CO_2 captured will be limited by the number of ions that can be move by these defects. When temperature exceeds 600 °C, new defects are generated and then the CO_2 captured will be limited by the number of ions that can migrate at that temperature. In this scenario, creating new defects enhances the capture but as some ions Li^{1+} and O^{2-} form other crystal phases, the remaining ions arrange to yield the $LiAlO_2$ phase. At $T > 700$ °C the CO_2 capture becomes constant, in this point all ions involved in the CO_2 captured are movable but only a portion are available to form Li_2CO_3, while the remains produce $LiAlO_2$ phase.

4. Conclusions

Penta lithium aluminate (Li_5AlO_4) was produced via a solid state reaction to study the CO_2 capture varying the CO_2 and O_2 partial pressures. Dynamic and isothermal thermogravimetric analyzes were used to evaluate the CO_2 chemisorption process, in the absence or presence of oxygen. Initially, the use of different CO_2 partial pressures (P_{CO_2} between 0.5 and 0.1) did not show important difference during the dynamic CO_2 chemisorption, in comparison to the CO_2 saturated atmosphere. Moreover, qualitatively, oxygen addition ($P_{O_2} = 0.05$) seemed to enhance the CO_2 chemisorption process at a certain temperature range. These results were corroborated with the corresponding kinetic analysis, showing that oxygen addition did improve the CO_2 capture. It was determined using a double exponential model.

Based on these results, an alkaline carbonate mixture was added to Li_5AlO_4 sample to modify the diffusion conditions due to the carbonate melting process. Results showed that the eutectic phase shifted to lower temperatures the CO_2 capture. Additionally, the analysis of the ionic conductivity of Li_5AlO_4 complemented this work. The ionic conductivity and activation energy of Li_5AlO_4 were determined, showing that the ionic conduction behavior change at around 600 °C. This result was is in good agreement with the previous thermogravimetric analyzes. Therefore, these results confirm the importance of the oxygen viability during the carbonation process of Li_5AlO_4.

Acknowledgments

This work was financially supported by the projects PAPIIT-UNAM (IN-101916) and SENER-CONACYT (251801). Authors thank to Adriana Tejeda for technical assistance. PSC and JFGG thank to CONACYT and DGAPA-UNAM for financial support.

References

[1] K. Oh-Ishi, Y. Matsukura, T. Okumura, Y. Matsunaga, R. Kobayashi, J. Solid State Chem. 211 (2014) 162–169.
[2] M. Puccini, E. Stefanelli, M. Seggiani, S. Vitolo, Chem. Eng. Trans. 47 (2016) 139–144.
[3] A. Iwan, H. Stephenson, W.C. Ketchie, A.A. Lapkin, Chem. Eng. J. 146 (2009) 249–258.
[4] M. Xie, Z. Zhou, Y. Qi, Z. Cheng, W. Yuan, Chem. Eng. J. 207–208 (2012) 142–150.
[5] X. Yang, W. Liu, J. Sun, Y. Hu, W. Wang, H. Chen, Y. Zhang, X. Li, M. Xu, ChemSusChem 9 (2016) 1607–1613.
[6] E. Ochoa-Fernández, T. Zhao, M. Rønning, D. Chen, J. Environ. Eng. 135 (2009) 397–403.
[7] H.K. Rusten, E. Ochoa-Fernández, H. Lindborg, D. Chen, H.A. Jakobsen, Ind. Eng. Chem. Res. 46 (2007) 8729–8737.
[8] R. Rodríguez-Mosqueda, H. Pfeiffer, J. Phys. Chem. A 114 (2010) 4535–4541.
[9] M. Nomura, T. Sakanishi, Y. Nishi, K. Utsumi, R. Nakamura, Ener. Procedia 37 (2013) 1004–1011.
[10] M. Seggiani, M. Puccini, S. Vitolo, Int. J. Greenh. Gas Control 5 (2011) 741–748.
[11] I.C. Romero-Ibarra, J. Ortiz-Landeros, H. Pfeiffer, Thermochim. Acta 567 (2013) 118–124.
[12] Y. Duan, H. Pfeiffer, B. Li, I.C. Romero-Ibarra, D.C. Sorescu, D.R. Luebke, J.W. Halley, Phys. Chem. Chem. Phys. 15 (2013) 13538–13558.
[13] L.M. Palacios-Romero, H. Pfeiffer, Chem. Lett. 37 (2008) 862–863.
[14] Y. Matsukura, T. Okumura, R. Kobayashi, K. Oh-Ishi, Chem. Lett. 39 (2010) 966–967.
[15] K. Nakagawa, J. Electrochem. Soc. 145 (1998) 1344–1346.
[16] H. Pfeiffer, P. Bosch, Chem. Mater. 17 (2005) 1704–1710.
[17] B.N. Nair, R.P. Burwood, V.J. Goh, K. Nakagawa, T. Yamaguchi, Prog. Mater. Sci. 54 (2009) 511–541.
[18] Q. Xiao, X. Tang, Y. Liu, Y. Zhong, W. Zhu, Chem. Eng. J. 174 (2011) 231–235.
[19] T. Avalos-Rendón, J. Casa-Madrid, H. Pfeiffer, J. Phys. Chem. A 113 (2009) 6919–6923.

[20] T. Avalos-Rendón, V.H. Lara, H. Pfeiffer, Ind. Eng. Chem. Res. 51 (2012) 2622–2630.
[21] S.M. Amorim, M.D. Domenico, T.L.P. Dantas, H.J. José, R.F.P.M. Moreira, Chem. Eng. J. 283 (2016) 388–396.
[22] Q. Feng, X. Xu, X. Zeng, G. Lv, J. Deng, W. Ma, Y. Zhou, Current Environ. Eng. 2 (2015) 127–131.
[23] S. Jeoung, J.H. Lee, Y. Kim, H.R. Moon, Thermochim. Acta 637 (2016) 31–37.
[24] Q. Guan, X. Chen, T. Gao, C. Xiao, L. Zhao, J. He, X. Long, J. Nucl. Mater. 465 (2015) 170–176.
[25] I. Alcérreca-Corte, E. Fregoso-Israel, H. Pfeiffer, J. Phys. Chem. C 112 (2008) 6520–6525.
[26] L. Martínez-dlCruz, H. Pfeiffer, Ind. Eng. Chem. Res. 49 (2010) 9038–9042.
[27] H.R. Radfarnia, M.C. Iliuta, Sep. Purif. Technol. 93 (2012) 98–106.
[28] H.G. Jo, H.J. Yoon, C.H. Lee, K.B. Lee, Ind. Eng. Chem. Res. 55 (2016) 3833–3839.
[29] Q. Xiao, Y. Liu, Y. Zhong, W. Zhu, J. Mater. Chem. 21 (2011) 3838–3842.
[30] M.T. Flores-Martínez, H. Pfeiffer, Greenh. Gas. Scien. Technol. 5 (2015) 802–811.
[31] J. Ortiz-Landeros, T. Norton, Y.S. Lin, Chem. Eng. Sci. 104 (2013) 891–898.
[32] S. Lowell, J.E. Shields, M.A. Thomas, M. Thommes, Characterization of Porous Solids and Powders: Surface Area, Pore Size and Density, Kluwer Academic Publishers, London, 2004.
[33] L. Martinez-dlCruz, H. Pfeiffer, J. Phys. Chem. C 116 (2012) 9675–9680.
[34] L. Lei, D. He, Z. Yongtao, W. Zhang, Z. Wang, M. Jiang, M. Du, J. Solid State Chem. 181 (2008) 1810–1815.
[35] J. Ortiz-Landeros, T.L. Ávalos-Rendón, C. Gómez-Yáñez, H. Pfeiffer, J. Therm. Anal. Calor. 108 (2012) 647–655.
[36] B. Alcántar-Vázquez, C. Diaz, I.C. Romero-Ibarra, E. Lima, H. Pfeiffer, J. Phys. Chem. C 117 (2013) 16483–16491.
[37] A. Peters, C. Korte, D. Hesse, N. Zakharov, J. Janek, Solid State Ion. 178 (2007) 67–76.
[38] T.V.S. L. Satyavani, B. Ramya-Kiran, V. Rajesh-Kumar, S.A. Kumar, S.V. Naidu, Eng. Sci. Technol. Int. J. 19 (2016) 40–44.
[39] R.J.D. Tilley, Defects in Solids, John Wiley & Sons, Inc., London, 2008.